AJNR Am J Neuroradiol 26:2128–2133, September 2005

Current Multiplanar Imaging of the Stapes

Philippe Henrot, Sandrine Iochum, Toufik Batch, Laurent Coffinet, Alain Blum, and Jacques Roland

PURPOSE: **CT analysis of the stapes is difficult in the axial plane (AP), because of its oblique orientation. Oblique axial reformations could provide a more precise analysis of the stapes in normal and pathologic conditions.**

MATERIALS AND METHODS: **CT of the temporal bone was performed in 31 patients. Only the normal side was examined in the AP and oblique axial plane (OAP), in the plane of the stapes superstructure. Conspicuousness of each stapes component was evaluated in both planes by 2 independent readers. Reproducibility between the 2 readers (R1 and R2) and comparison of conspicuousness between the AP and the OAP in the analysis of the stapes crura were evaluated. The normal position of the stapes arch in relationship to the footplate was determined in the OAP by using biometric landmarks.**

RESULTS: **Conspicuousness of the stapes crura was increased by using OAP. The conspicuousness of the anterior crus was enhanced in 38% with the OAP according to R1 ($P < .05$) and 32% according to R2 ($P < .05$). The conspicuousness of the posterior crus was enhanced in 35% with the OAP according to R1 ($P < .05$), but not significantly enhanced in 22% with the OAP according to R2 ($P = .095$). Analysis of conspicuousness of the stapes crura was reproducible according to the kappa test.**

A perpendicular line to the footplate intersecting its midportion crosses the stapes head and the long process of the incus in the OAP in normal patients.

CONCLUSION: **OAP could enhance the CT analysis of the stapes and provide useful biometric landmarks in pathologic conditions.**

The stapes is the smallest bone of the human body. It features a link transmitting vibrations from the aerial environment of the middle ear to the liquid environment of the inner ear. It can be involved by trauma, infection, or malformation, resulting in a conductive hearing loss.

Imaging of the stapes is a challenge because of the very small size of its components, the head, the crura, and the footplate. Imaging findings of stapes in pathologic conditions have been described in the axial plane (AP) parallel to the infraorbital-meatal line or to the palate and in a coronal plane nearly perpendicular to the AP (1–3). In these planes, only fractional portions of the stapes are visible per section, because the footplate is actually oblique in relationship to the axial and coronal scan planes. In the AP, the upper sections only depict the medial portion of the stapes crura, and the lower sections only depict the incudostapedial joint area. Consequently, a fracture of the crura or a displacement of the stapes superstructure could be overlooked. In the coronal plane, a V-shaped continuity is observed between the long process of the incus, the lenticular process of the incus, the incudostapedial joint, and the only crus that lies in the coronal plane, the anterior crus; therefore, a minor displacement of the ossicular chain remains difficult to detect in this plane.

The diagnosis of stapes injury can be reported with indirect signs, when the stapes superstructure is not visualized in the oval window niche in the coronal plane (1). Direct signs of lesions, as well as a fracture of 1 or 2 stapes crura on axial CT, have also been reported but are difficult to assess, because of a low contrast, the oblique orientation, and the occurrence of normal dehiscence.

The enhanced multiplanar performance of current multisection CT yields reconstructed images in any plane with a spatial resolution comparable to that of axial native sections. In many institutions, coronal reformation from axial CT data has replaced direct coronal CT scan (4, 5). The interest of nonorthogonal

Received October 26, 2004; accepted after revision February 24, 2005.

From the Department of Radiology, Centre Alexis Vautrin, Avenue de Bourgogne, Vandoeuvre-les-Nancy, France (P.H.); and the Departments of Radiology Guilloz (P.H., S.I., T.B., A.B., J.R.) and Head and Neck Surgery (L.C.), CHU Nancy, University of Nancy, Nancy, France.

Address correspondence to P. Henrot, MD, Department of Radiology, Centre Alexis Vautrin, Avenue de Bourgogne, 54511 Vandoeuvre-les-Nancy, France.

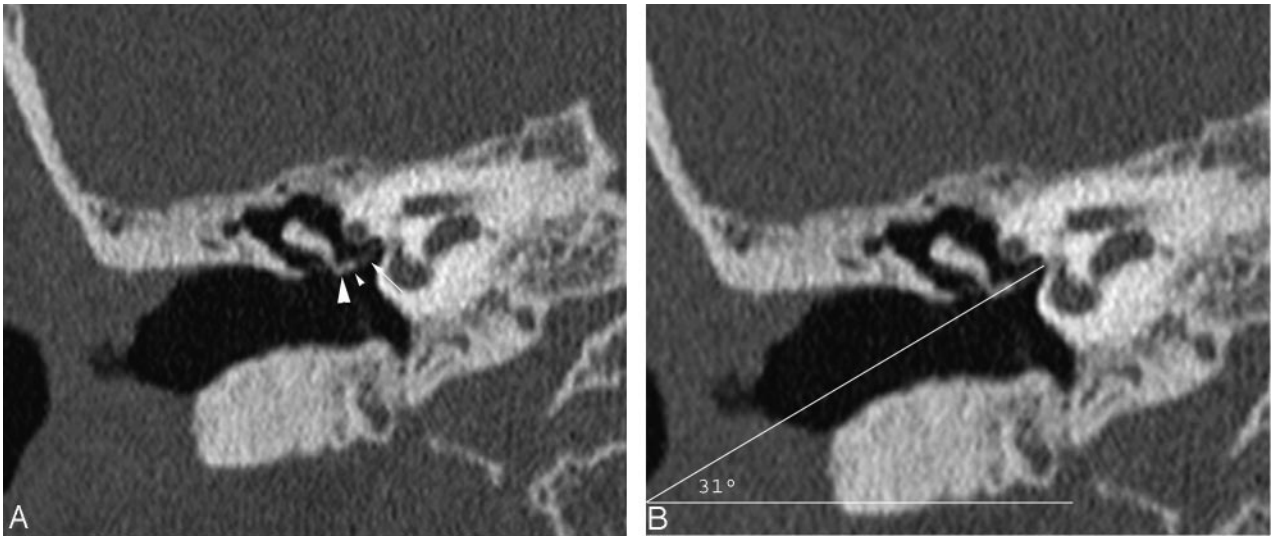

FIG 1. Coronal reformation demonstrating the stapes superstructure. *A,* The anterior crus (*small arrow*), the stapes head (*small arrowhead*), and the lenticular process of the incus (*large arrowhead*) are distinctly depicted, forming a "V" with the long process of the incus. The oblique axial images are reformatted in this plane. *B,* The angle between the OAP and the AP is 31° in this example.

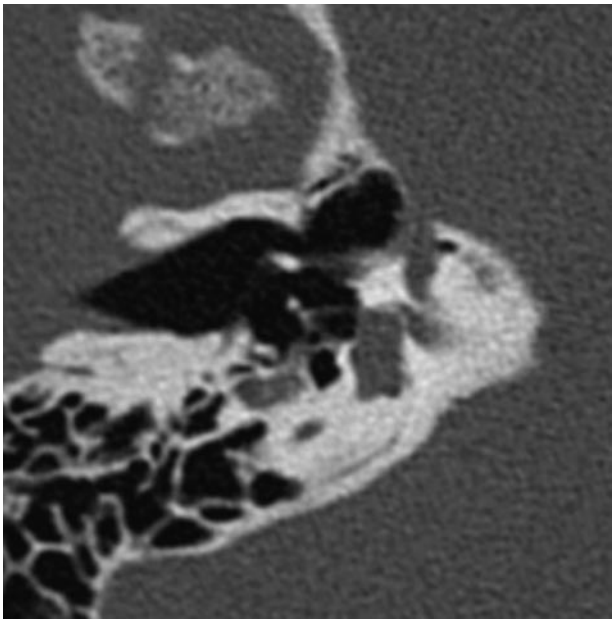

FIG 2. Oblique axial reformation in the plane of the stapes superstructure. All components of the stapes—the head, the crura, and the footplate—are depicted on a single view.

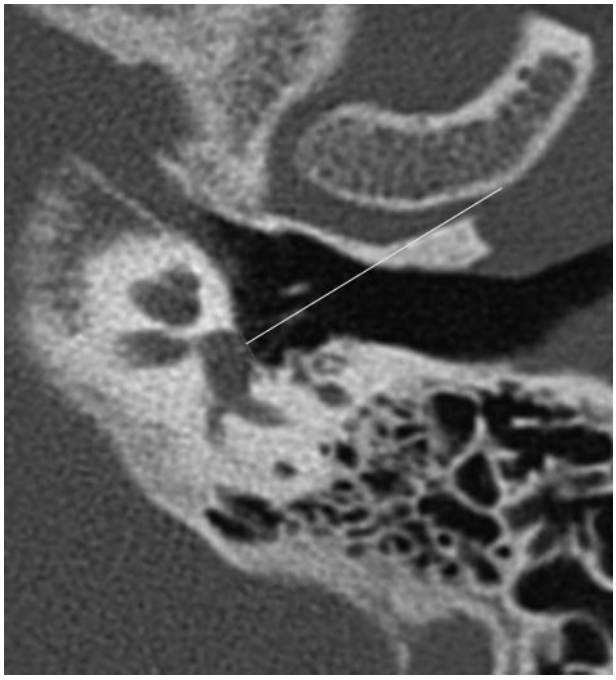

FIG 3. Angle between the plane of the footplate and the S-line intersecting the midportion of the footplate and crossing the stapes head. In this example the angle is 88.3°. The S-line also crosses the long process of the incus.

view of the temporal bone has been reported in the planning of surgery (6). In the particular case of the stapes, its small size associated with its oblique orientation makes the multiplanar reformation especially useful. State-of-the-art CT technology could highlight the entire stapes in a reformated oblique axial plane (OAP) with a spatial resolution similar to that of axial or coronal images.

Methods and Materials

CT examination of the temporal bone was performed in 31 consecutive adult patients for various diseases, including complicated chronic otitis or deafness. Only the normal side was examined in this study. The acquisition consisted of 16 rows of 0.75-mm sections at 120 kV and 250 mAs or 2 rows of 0.6-mm sections at 120 kV and 330 mAs (Sensation 16; Siemens, Erlangen, Germany). The mean dose length product was 500 ± 66 mGy/cm. Reformatted images consisted of overlapped axial sections of 0.75 mm every 0.5 mm or 0.6 every 0.4 mm, respectively, in the infraorbital meatal plane. These sections were reformatted with a dedicated workstation (Voxar 3D, Edinburgh, Scotland) in the coronal plane and in an OAP through both crura and capitellum of the stapes.

The plane of the stapes superstructure was determined by using the coronal section demonstrating the stapes anterior crus in the oval window niche, and the oblique axial reformations were performed in this plane (Figs 1 and 2). The inclina-

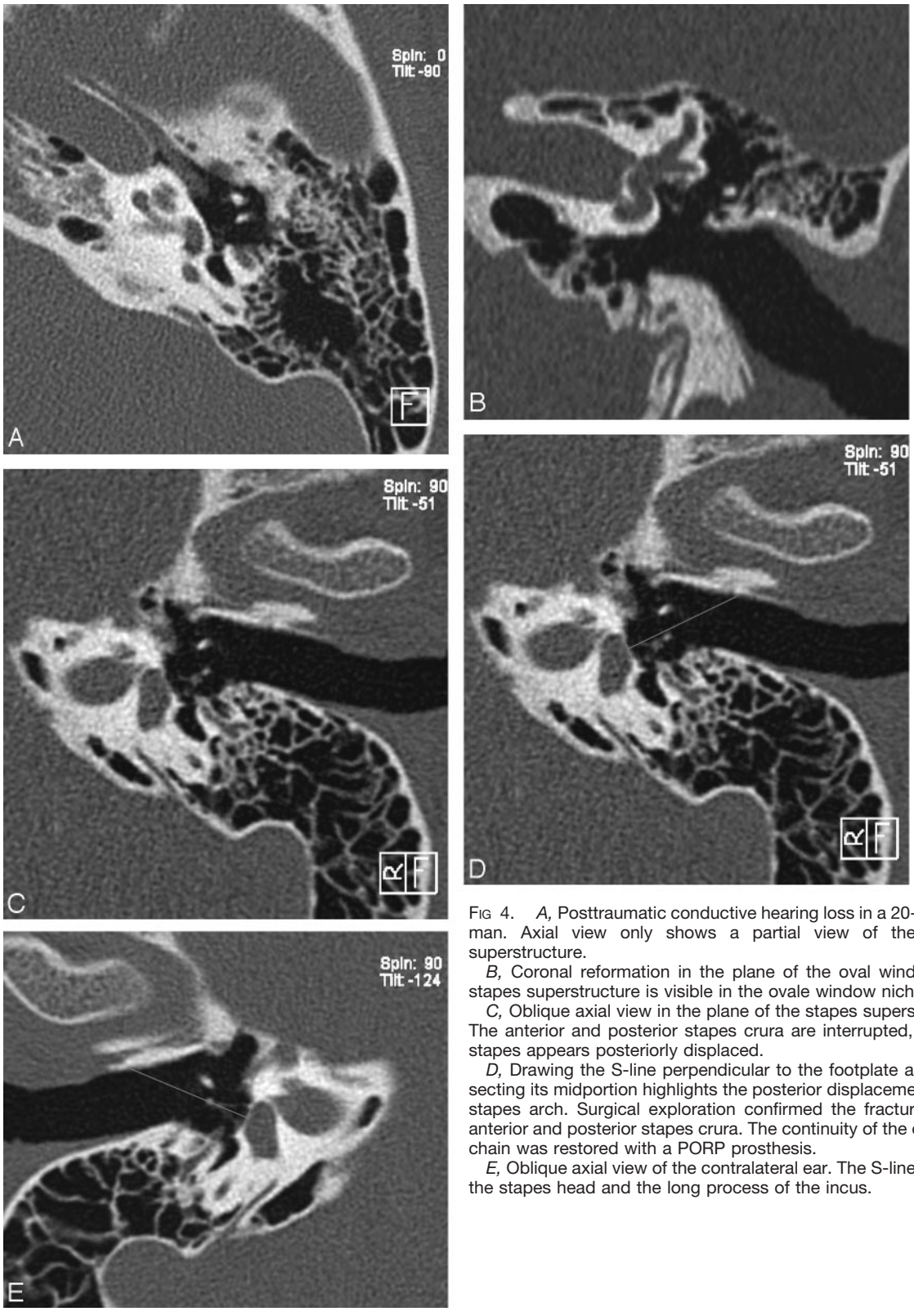

FIG 4. *A,* Posttraumatic conductive hearing loss in a 20-year-old man. Axial view only shows a partial view of the stapes superstructure.

B, Coronal reformation in the plane of the oval window. The stapes superstructure is visible in the ovale window niche.

C, Oblique axial view in the plane of the stapes superstructure. The anterior and posterior stapes crura are interrupted, and the stapes appears posteriorly displaced.

D, Drawing the S-line perpendicular to the footplate and intersecting its midportion highlights the posterior displacement of the stapes arch. Surgical exploration confirmed the fracture of the anterior and posterior stapes crura. The continuity of the ossicular chain was restored with a PORP prosthesis.

E, Oblique axial view of the contralateral ear. The S-line crosses the stapes head and the long process of the incus.

tion of this OAP was measured on the former coronal image by drawing a line extending along the visible crus and a horizontal line featuring the actual AP (Fig 1).

The conspicuousness of the incudostapedial joint, the stapes head, the stapes anterior and posterior crura, and the footplate was rated by 2 independent reviewers (R1 and R2). A good view was scored 1; acceptable view, 2; poor view, 3; and non-visible structure, 4. Mean values and standard deviations were measured for each structure in the AP and in the OAP.

The percentage comparison of the conspicuousness of anterior crus and posterior crus by both axial and oblique axial images was made with a paired χ^2 test for the 2 readers.

Interobserver reproducibility of the conspicuousness of the stapes crura was evaluated by the kappa agreement test.

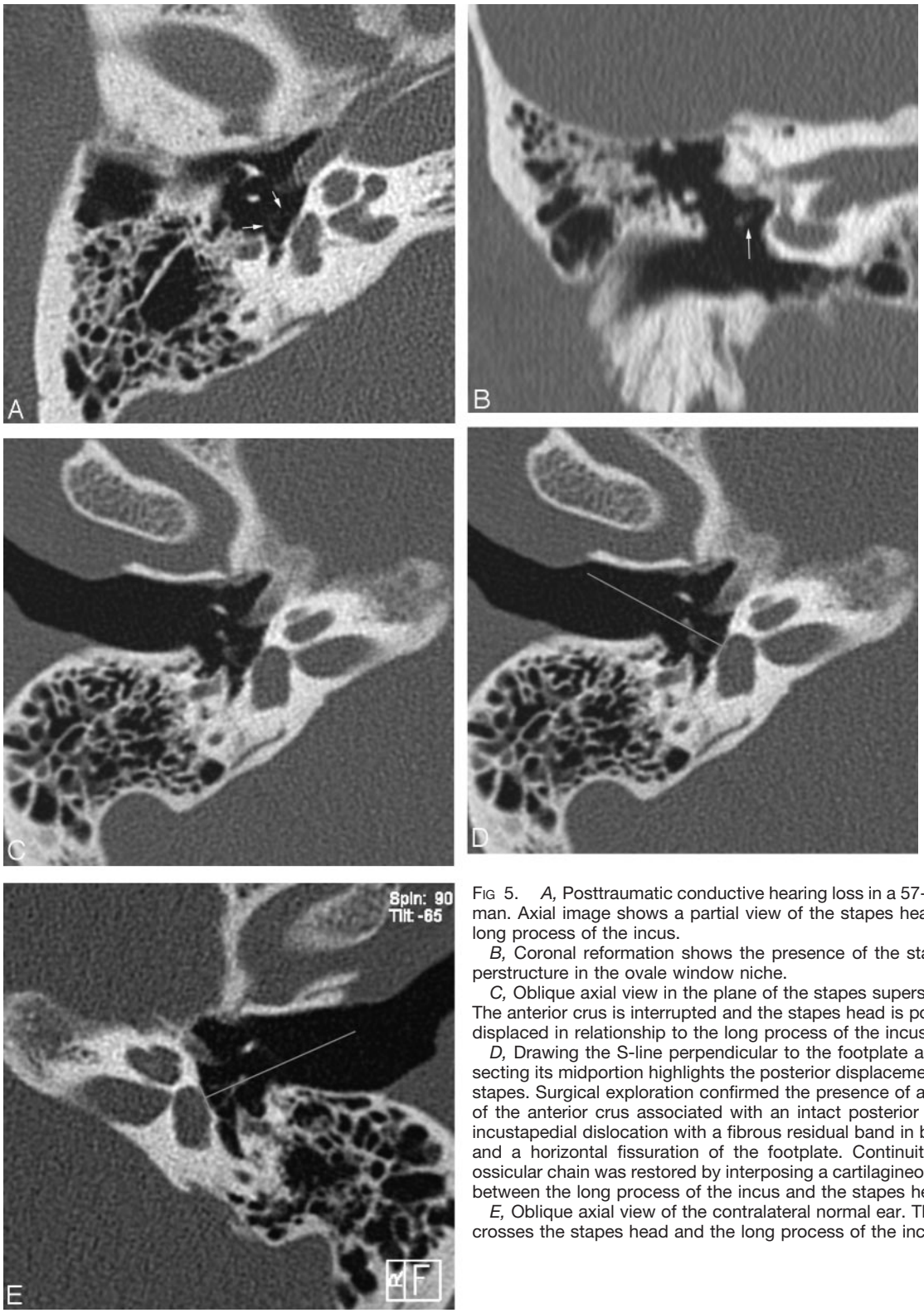

FIG 5. *A,* Posttraumatic conductive hearing loss in a 57-year-old man. Axial image shows a partial view of the stapes head of the long process of the incus.

B, Coronal reformation shows the presence of the stapes superstructure in the ovale window niche.

C, Oblique axial view in the plane of the stapes superstructure. The anterior crus is interrupted and the stapes head is posteriorly displaced in relationship to the long process of the incus.

D, Drawing the S-line perpendicular to the footplate and intersecting its midportion highlights the posterior displacement of the stapes. Surgical exploration confirmed the presence of a fracture of the anterior crus associated with an intact posterior crus, an incustapedial dislocation with a fibrous residual band in between, and a horizontal fissuration of the footplate. Continuity of the ossicular chain was restored by interposing a cartilagineous patch between the long process of the incus and the stapes head.

E, Oblique axial view of the contralateral normal ear. The S-line crosses the stapes head and the long process of the incus.

The position of the stapes superstructure in relationship to the footplate was analyzed in the OAP in each patient. The middle of the footplate was determined and the angle formed by the plane of the footplate and the line crossing the middle of the footplate, and the stapes head was measured in the population of the study (Fig 3).

Results

The mean angle of the stapes superstructure in the coronal plane in relationship to the AP was 32.8° ± 6.83.

Scores of conspicuousness according to the 2 readers (R1 and R2) are reported in Table 1.

Conspicuousness according to independent readers R1 and R2

	ISJ	SH	AC	PC	F
R1					
Axial	1.09 ± 0.3	1.32 ± 0.59	1.61 ± 0.61	1.51 ± 0.62	1
Oblique axial	1.09 ± 0.3	1.06 ± 0.24	1.12 ± 0.34	1.12 ± 0.34	1.03 ± 0.03
R2					
Axial	1.09 ± 0.3	1.32 ± 0.59	1.41 ± 0.62	1.38 ± 0.61	1
Oblique axial	1.09 ± 0.3	1.09 ± 0.3	1.03 ± 0.03	1.16 ± 0.37	1

Note.—Values are mean scores (±SD). ISJ indicates incudostapedial joint; SH, stapes head; AC, anterior crus of the stapes; PC, posterior crus of the stapes; F, footplate.

The conspicuousness of the incudostapedial joint was scored 1.09 ± 0.30 by R1 and 1.09 ± 0.30 by R2 in the AP and 1.09 ± 0.30 by R1 and 1.09 ± 0.30 by R2 in the OAP.

The conspicuousness of the stapes head was scored 1.32 ± 0.59 by R1 and 1.32 ± 0.59 by R2 in the AP and 1.06 ± 0.24 by R1 and 1.09 ± 0.3 by R2 in the OAP.

The conspicuousness of the anterior crus was scored 1.61 ± 0.61 by R1 and 1.41 ± 0.62 by R2 in the AP and 1.12 ± 0.34 by R1 and 1.41 ± 0.62 by R2 in the OAP.

The conspicuousness of the posterior crus was scored 1.51 ± 0.62 by R1 and 1.38 ± 0.61 by R2 in the AP and 1.12 ± 0.34 by R1 and 1.38 ± 0.61 by R2 in the OAP.

The conspicuousness of the footplate was scored 1 by R1 and 1 by R2 in the AP and 1.03 ± 0.3 by R1 and 1 by R2 in the OAP.

The conspicuousness of the anterior crus was enhanced in 38% with the OAP according to R1 ($P < .05$) and 32% according to R2 ($P < .05$).

The conspicuousness of the posterior crus was enhanced in 35% and decreased in 3% with the OAP according to R1 ($P < .05$). It was enhanced without statistical significance in 22% and decreased in 6% with the OAP according to R2 ($P = .095$).

Kappa agreement test between R1 and R2 in the analysis of the anterior crus was good in the AP ($\kappa = 0.70$, with a percentage of agreement of 0.83) and middle in the OAP ($\kappa = 0.37$, with a percentage of agreement of 0.90). In the analysis of the posterior crus, kappa agreement test between R1 and R2 was good in the AP ($\kappa = 0.75$, with a percentage of agreement of 0.87) and excellent in the OAP ($\kappa = 0.86$, with a percentage of agreement of 0.96).

The angle formed by the plane of the footplate and a line crossing the stapes head and the middle of the footplate was 90.86° ± 3.16. This line also crosses or is in contact with the long process of the incus.

Discussion

In this study, the use of an OAP does not yield a significantly better conspicuousness of the incudostapedial joint, the footplate, and the stapes head (Table 1). In fact, the footplate and the stapes head are quite easy to depict in the AP without the need for reformation. The depiction of the actual incudostapedial joint, however, could be controversial, because the small gap between the lenticular process and the long process could be labeled uncudostapedial joint on the axial images. The OAP through the stapes superstructure could feature the nearest approach to the actual incudostapedial joint in the plane of the lenticular process (Fig 1).

The conspicuousness of the stapes crura appears to be consistently enhanced (Table 1), according to the oblique orientation of the stapes superstructure relative to the AP (32.8° ± 6.83 in this study).

The middle reproducibility of the interobserver analysis of the anterior crus could probably be due to the fact that the anterior crus is smaller than the posterior crus. Another explanation could be the level of image noise that could decrease the image quality. We chose dose parameters as low as possible, enabling visualization of thin structures such as stapes crus. A compromise between image quality and radiation dose should be adjusted to the pathologic process and the intrinsic qualities of the CT. In the case of a complicated chronic otitis, a low-dose examination seems sufficient to detect a cholesteatoma. The depiction of otosclerosis or stapes trauma, however, requires less noise and more contrast and, therefore, a higher dose. We explored only temporal bones in adults in this study, by using a classic reported protocol in the orbital-meatal plane. In children, the radiation dose, especially to the lens, could be reduced by performing CT at 25° angle to the Reid baseline or on the coronal plane with reformatted axial images. Another explanation of the interobserver variability could be the unavoidable minor angular variations in setting reformatted images in the plane of the stapes crura between several operators.

The OAP is able to display on the same image the footplate and the entire stapes superstructure. Therefore, it can demonstrate the normal position of the stapes superstructure in relationship to the footplate and to the long process of the incus. This study reports that a line, intersecting the midportion of the footplate and crossing the stapes head, is mostly aligned perpendicular to the plane of the footplate. Moreover, this line crosses or is in contact with the long process of the incus. Using this S-line could facilitate the depiction of some minor lesions of the ossicular chain, such as isolated stapes displacement and minor incudostapedial dislocation. The classic reported sign of a stapes fracture is the nonvisibility of the stapes superstructure in the ovale window niche in the coronal plane. Rarely, some bony mate-

rial and gas in the vestibule demonstrate a stapedovestibular dislocation. Some more subtle lesions such as fractures of 1 or 2 stapes crura are more difficult to depict and could mimic simple dehiscence. The depiction of a minor displacement of the stapes associated with a stapes discontinuity could demonstrate a fracture of the ossicular chain. We report as examples 2 cases of surgically proved fracture of the stapes crura associated with a posterior displacement of the stapes relative to the S-line (Figs 4 and 5). The displacement mechanism is presumed to result from the contraction of the stapedius muscle attached anywhere from the incudostapedial region to the junction of the posterior crus with the footplate. The sudden contraction of the stapedius muscle occurring at the time of the head trauma might even be responsible for the stapes fractures (7).

Conclusion

The use of oblique axial reformation with current multisection CT could demonstrate minor abnormalities of the stapes. Minor displacement or fracture of the stapes crura as well as minor incudostapedial dislocation could be highlighted by analyzing biometric landmarks yielded by this technique. The clinical interest of these reformations in routine CT examination of conductive hearing loss could be investigated in a larger study.

References

1. Meriot P, Veillon F, Garcia JF, et al. **CT appearances of ossicular injuries.** *Radiographics* 1997;17:1445–1454
2. Swartz JD, Swartz NG, Korsvik H, et al. **Computerized tomographic evaluation of the middle ear and mastoid for posttraumatic hearing loss.** *Ann Otol Rhinol Laryngol* 1985;94:263–266
3. Lemmerling MM, Stambuk HE, Mancuso AA, et al. **Normal and opacified middle ears: CT appearance of the stapes and incudostapedial joint.** *Radiology* 1997;203:251–256
4. Venema HW, Phoa SSKS, Mirck PGB, et al. **Petrosal bone: Coronal reconstructions from axial spiral CT data obtained with 0.5-mm collimation can replace direct coronal sequential CT scans.** *Radiology* 1999;213:375–382
5. Caldmeyer KS, Sandrasegaran K, Shinaver CN, et al. **Temporal bone: comparison of isotropic helical CT and conventional direct axial and coronal CT.** *AJR Am J Roentgenol* 1999;172:1675–1682
6. Manolidis S, Williamson B, Chan LL, et al. **Use of reconstructed, non-orthogonal plane, high-resolution computed tomography of the temporal bone in the planning temporal bone surgery.** *ORL J Otorhinolaryngol Relat Spec* 2003;65:71–75
7. Swartz JD, Harnsberger HR. *Imaging of the temporal bone.* 3rd ed. New York: Thieme;1998:332